Congr. Int. en Ing. Electrónica. Mem. ELECTRO, Vol. 39, pp. 120-128, Oct 2017, Chihuahua, Chih. México
http://electro.itchihuahua.edu.mx/memorias_electro/MemoriaElectro2017.zip
ISSN 1405-2172

MODELING SIMULTANEOUS ED/PEC IN LOW-RESISTIVITY DEIONIZED WATER (LR-DW) FOR MACHINING HSLA STEEL USING HIGH-FREQUENCY PULSED SOURCE

Orona-Hinojos J.M.[1*], Álvarez-Vera M.[2], Hurtado Delgado Eduardo[2], Macias-Avila Eduardo[3], Granda-Gutiérrez Everardo E.[4], Pérez Villanueva Pedro[2]

[1]QUIMMCO Innovación, Av. Roble No. 701, Valle del Campestre, San Pedro García N.L. CP 66265, México
[2]COMIMSA, Ciencia y Tecnología No. 790, Saltillo 400, Saltillo Coah., C.P. 25290, México.
[3]Centro de Ingeniería y Desarrollo Industrial, Apodaca N.L., C.P. 66626, México.
[4]Universidad Autónoma del Estado de México (UAEM). Toluca, C.P. 50110, Estado de México.

e-mail * jesus.orona@quimmco.com

RESUMEN

La influencia del mecanizado electroquímico pulsado (PECM) durante un proceso activo de electro descarga (EDM) sobre la superficie de corte de una pieza de trabajo, es combinada como un proceso hibrido novedoso denominado maquinado simultáneo ED/PEC. Este estudio evalúa los parámetros de mecanizado en el barrenado de un acero de alta resistencia HSLA, utilizando S-ED/PEC en un medio de agua des-ionizada de baja resistividad. Se propone la correlación de un modelo matemático para determinar la tasa de remoción de material (MRR) y la proporción de energía transferida. La energía de la chispa se realiza a corrientes de 15A y 25A, durante periodos de descarga activos de 12 a 28 µs, usando una fuente pulsada de 25 KHz. Los resultados revelan una diferencia sustancial en la remoción de material. La condición PECM permitió la remoción por disolución de metal posterior a la descarga, reduciendo la zona afectada por el calor, resultando en un MRR mayor de acuerdo con la predicción del modelo.

Palabras Clave: Electro-descarga EDM, Maquinado electroquímico-Pulsado PECM, energía transferida

ABSTRACT

The influence of pulsed electrochemical machining (PECM) on a simultaneous pulsed train of discharge plasma energy from electrical discharge machining (EDM) on the surface of a workpiece combined with presents a hybrid machining process, namely simultaneous ED/PEC drilling. This combine electro discharge and chemical machining in low-resistivity deionized water was investigated to obtain an experimental material removed rate (MRR) using transferred energy to the workpiece during an active discharge period of On-time 12 to 28 µs. A mathematical model correlation is proposed to determine the MRR and proportion of transferred energy for each individual process when drilling holes in high-strength steel (HSS). The spark energy was performed between 15A and 25A. The results revealed a substantial difference in the recasting of white-layers after the sparking cycle in EDM drilling. The PECM condition allowed the material removal mechanism using metal dissolution reducing the heat affected zone during hybrid S-ED/PEC, resulting in a higher removal rate according to the modeling prediction.

Keywords: Simultaneous EDPEC machining, high frequency pulsed EDM, transferred energy.

Abbreviations.

α	Symmetry factor
$\beta_{a,Fe}$	TAFEL anodic constant $[mV^{-1}]$
δ	Tooling thickness (µm)
η_{Fe}	Anodic over potential of iron $[mV]$
$\phi_{a,Fe}$	Anodic potential of iron $[mV]$
ϕ^0	Standard potential $[mV]$
$i_{o,Fe}$	Current of ion-exchange of iron $[A]$
φ	Volume fraction by cycle
ψ_s	Energy share factor ED
ψ_d	Energy share factor EC
$\Delta t_{on,ED}$	Active differential time for ED $[s]$
$\Delta t_{on,EC}$	Active differential time for EC $[s]$
A_T	Drilling area [mm^2]
DW	Deionized water dielectric
LR-DW	Low-resistivity deionized water
EC	Electrochemical process
ED	Electrodischarge process
S-ED/PEC	simultaneous ED/CM drilling
$E(t)$	Energy transferred $[J \cdot cycle^{-1}]$
E_d	Energy transferred for EC $[J \cdot cycle^{-1}]$
E_s	Energy transferred for ED $[J \cdot cycle^{-1}]$
E_h	Energy transferred for SEDCM hybrid $[J \cdot cycle^{-1}]$
f_e	Factor of equivalent current
F	Faraday constant $[C \cdot mol^{-1}]$

F_{in}	LR-DW/DW internal flow $[mm^3 \cdot min^{-1}]$
F_{out}	LR-DW outside flow $[mm^3 \cdot min^{-1}]$
I_e	Current wave equivalent $[A]$
I_F	Faraday current $[A]$
I_p	Current of wave peak $[A]$
K_m	Machinability constant $[mm^3 \cdot m^{-2} \cdot J^{-1}]$
K_d	Machinability constant for EC $[mm^3 \cdot m^{-2} \cdot J^{-1}]$
K_s	Machinability constant for ED $[mm^3 \cdot m^{-2} \cdot J^{-1}]$
K_h	Machinability constant SED/PEC$[mm^3 \cdot m^{-2} \cdot J^{-1}]$
MRR^p	Planar material removal rate $[mm^3 \cdot m^{-2} \cdot s^{-1}]$
MRR_d^p	Planar material removal rate EC $[mm^3 \cdot m^{-2} \cdot s^{-1}]$
MRR_s^p	Planar removal rate for ED $[mm^3 \cdot m^{-2} \cdot s^{-1}]$
MRR_s	Material removal rate for ED $[mm^3 \cdot min^{-1}]$
MRR_{hyb}	Material removal rate for SEDCM $[mm^3 \cdot min^{-1}]$
R	Ideal gases constant $[J \cdot mol^{-1} \cdot K^{-1}]$
R_m	Average radius [µm]
S_o	Tooling-workpiece gap $[mm]$
t_c	Cycle time $[s]$
t_i	Iterative time $[s]$
t_{on}	On-time $[s]$
t_{off}	Off-time $[s]$
T	Temperature $[K]$
V_a	Anodic voltage $[mV]$
V_s	Pulsed voltage of source $[V]$
VR	Removal volume rate $[mm^3]$
VR_d	Removal volume rate for ED dissolution $[mm^3]$
VR_s	Removal volume rate for ED spark $[mm^3]$
z_0	Initial reference z-axis
z	Numbers of electrons exchange-redox

1. INTRODUCCIÓN

The non-conventional simultaneous ED/PEC drilling is a newly developed hybrid machining that consists of electrical discharge machining (EDM) and pulsed electrochemical machining (PECM), with a particular focus on establishing good stability and developing a relatively easy configuration system that combines an ion-plasma phenomenon. ED/EC hybrid has application advantages in the manufacturing field such as deep hole drilling and the finishing of precision parts. Rajurkar et al. [1] analyzed the influence of EDM and ECM as an alternative in generating accurate complex shaped macro, micro and nano features and components of difficult-to-machine materials. Pawar et al. [2] defined a novel theoretical model Electro chemical discharge machining of micromachining in non-conducting hard and brittle materials such as glass, ceramics and composites. Wang et al. [3] stablished a counter-rotating electrochemical machining (CRECM) as a new ECM technique which can be used to fabricate convex structures on thin-walled revolving parts. Several machining processes have been combined with EDM to enable improved machining characteristics such as ultrasonic vibrations forming hybrid (UEDM), which improves the material removal rate as was reported by Zhang et al. [4]. In the same way, when combining the hybrid ternary electrochemical discharge grinding (ECDG) process, the MRR improves considerably, such as described by El-Hofy [5]. Singh and Dvivedi [6], classified the ED/EC hybrid process developed EDCM based triplex hybrid methods as primary and secondary processes. The mixing of third energy with EDCM via tool rotations or addition of powders in electrolyte is termed as primary hybridization. Further, the material removal caused by the assistance of mechanical or magnetic forces are termed as the secondary hybrid processes.

The combination of the EDM and ECM processes has the capability to produce highly complex and precise results for 3D-structure machining [1,6]. Conversely, the simultaneous micro ED/EC milling integrates advantages of each machining process to produce healthy microstructures on steel hardness with lower residual stress and a low surface roughness close to 40 nm, as found by Nguyen et al. [7]. The hybrid ED+EC has two variants, namely, i) electrolysis-based ECDM, which has been used in machining electrically conductive to non-conductive materials was proposal for the first time in 1968 and ii) simultaneous electro-discharge-chemical machining SEDCM in a semi-dielectric medium, such as low-resistivity in deionized water (LR-DW). Recent studies by Nguyen et al. [8] have determined that SEDCM milling to low-resistivity deionized water has the properties of a dielectric as well as slight conductive fluid that enables a weak electrochemical reaction during machining in the range of 0.1 to 0.5 MΩ·cm to remove material via electrical discharge and ionic dissolution.

The main characteristic of the S-ED/PEC hybrid process is an increase in material removal efficiency, as indicated by a higher MRR and a reduction in surface roughness, thereby providing a better finish surface as a consequence of the ECM process. It is well known that the EDM process significantly contributes to the MRR as it produces a heat affect zone (HAZ). Levy and Maggi [9] performed a study on W-EDM for the machining of heat treated high quality alloyed steels. They reported that the HAZ and the solidified layer reach 25 µm. Xiao-Lei et al. [10] reported a HAZ as white-layer of about 10 µm with high hardness. Zhao et al. [11] described a novel low cost, high efficiency material removal process namely the Blasting Erosion Arc Machining (BEAM). The material removal rate of the BEAM process is extremely higher regarding to traditional EDM. However, thickness of the HAZ caused by BEAM is

close to 200 µm. Further, the depth of the HAZ and the annealed layer is proportional to the amount of power used. That said, the wire EDM process significantly reduces the HAZ as reported by Newton et al. [12]. Zhang et al. [13] found that the hybrid machining technique of tube electrode high-speed electrochemical discharge drilling (TEHECDD) with thin thickness is free of recast layers and surface defects. The MRR during S-ED/PEC drilling in a low-resistivity dielectric condition results in electrical discharge and ionic dissolution, but the contributions of the EDM and ECM processes are not fully explained. In the preset work, a mathematical model is proposed for the simultaneous ED/EC drilling to determine the removal rate and the proportion of transferred energy at specific depths of white-layer to determine the contribution of each process when drilling holes in a high strength steel (HSS).

2. THEORETICAL MODEL OF SIMULTANEOUS ED/PEC

2.1 Simultaneous ED/PEC Drilling

The experimental scheme presents of Fig. 1 show the simultaneous ED/EC drilling condition. The S-ED/PEC machining combines electro-thermal discharge with electro-ionic dissolution, as indicated Fig. 1 (a). The pulsed signal is divided in two on-time conditions for the S-ED/PEC process, as in Fig. 1 (b). The pulsed signal is considered to increase the MRR assuming there is support of both processes. The physical chemical activation of the metallic surface condition by combining advantages constitutes the necessary support. Therefore, for electrochemical discharge machining requires the removal of material using a detachment surface mechanism to enhance the MRR. In this regard, Cheng-Kuang et al. [14] found an enhancement efficiency using a tool electrode with a spherical end that reduces the contact area between the electrode and the workpiece, thus facilitating the flow of electrolyte to the electrode end, resulting in efficient micro-hole drilling.

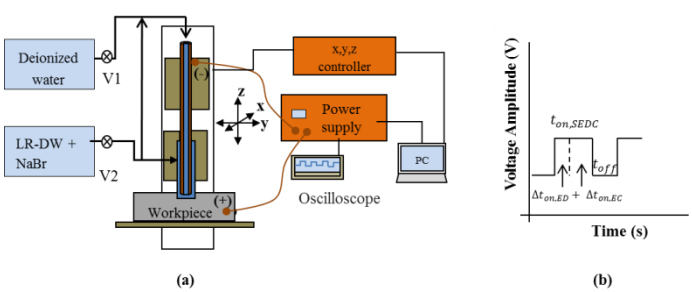

Fig. 1. Experimental scheme for (a) the simultaneous ED/EC condition (b) the pulsed signal for the S-ED/PEC.

Fig. 2 presents the tooling-workpiece scheme for the S-ED/PEC hybrid. There are irregular layers of micro thickness located on the active region due to the electro-discharge of the EDM, as noted in Fig. 2a. There are three main layers on the z_o surface after discharge. These layers include the i) melting pool layer, ii) recast layer (white-layer) and iii) heat affected zone. Fig. 2b presents the second material removal mechanism involves the release of an atomic layer, which is due to the electro-ionic dissolution process of ECM [15]. Thus, the material removal rate per unit area MRR^p $[mm^3 \cdot m^{-2} \cdot s^{-1}]$ is proportional to the energy function of the cycle $E(t)$ $[J \cdot cycle^{-1}]$ that is required for machining. As a result, a machinability constant, K_m $[mm^3 \cdot m^{-2} \cdot J^{-1}]$, also reported by Kozak et al. [16], is defined as in equation (1)

$$MRR^p * t = K_m * E(t) \tag{1}$$

However, in the case of SEDCM, the challenge is to estimate the amount of energy required for each ED and EC for a determined MRR that can then be quantified for each subsystem that involves the total material removal of drilling process.

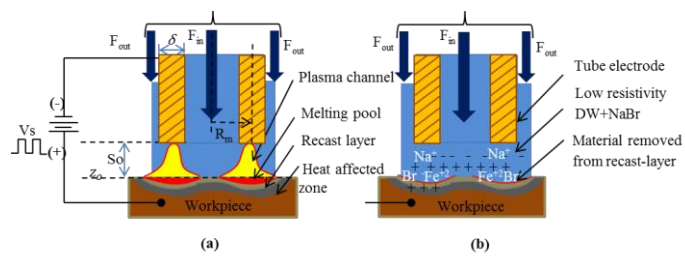

Fig. 2. Schematic tooling-workpiece for S-ED/PEC drilling under two-pulsed times divided as (a) Δt_{on1} for ED and (b) Δt_{on2} for EC.

The square waveform of the pulsed electrical signal of Simultaneous ED/PEC is displayed in Fig. 3. The S-ED/PEC drilling requires a pulsed power source, but it was difficult to achieve that a current with a magnitude that can be adjusted as an exact square waveform, as presented in Fig. 3 (a). Thus, Fig. 3 (b) presents the deformed wave current that is above the control value such that there exist a peak in the current, which is known as the attack region. This is followed of a decline below the desired value, which is an affected behavior of the external system, i.e., electronic performance, dielectric medium, workpiece materials [17].

A direct correlation exists between the amount of energy required by the EDM system and the MRR as determined by the discharge voltage magnitude V_s (Volts) and the average current Ie (A) as reported by Tao et al. [18], where the equivalent current can be obtained from the peak current average using a factor as in equation (2). This is observed in Fig. 3 (b) where the fitting signal is adjusted to an equivalent

current of the pulsed signal. The integral can be solved by equation (3) to determine the average sparking energy of the EDM process, as in Fig. 3 (c).

$$I_e = f_e * I_p \tag{2}$$

$$E_s = \int_0^{ton} Ie * V_s \, dt \tag{3}$$

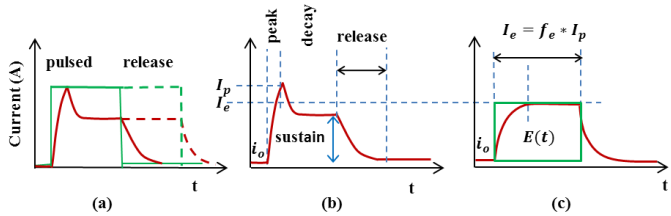

Fig. 3. Waveforms of a pulsed signal: (a) adjusted square waveform, (b) overcompensated peak signal and (c) undercompensated adjusted signal.

With respect to ECM and the energy of the simultaneous ED/EC drilling, it is well known that there is a nominal current i_o (A) of ion-exchange impulsed by an f.e.m. (force-electromotrice), which is considered polarization voltage of the tool-workpiece that allows for the redox electrochemical reaction studied by Graver and Moreland [19]. Then, the pulsed period with polarization anodic voltage V_a that is fed by a power source in the electrolyte medium generates ion dissolution via a transferred electrical charge, thereby producing a Faraday current I_F (A). The energy required to produce the dissolution of metal at the anodic-workpiece surface and is represented in equation (4) [16].

$$E_d = \int_0^{ton} I_F V_a \, dt \tag{4}$$

where V_a is the anodic voltage (volts) and I_F is the Faraday current (A) that can be determined using TAFEL equation (5) [19].

$$I_F = i_{o,Fe} * e^{\left(\propto \frac{zf}{RT}\right) * \eta_{Fe}} dt \tag{5}$$

$i_{o,Fe}$ is the ion-exchange current (A) and $\eta_{Fe} = (\phi_{a,Fe} - \phi^0)$ is the over potential (volts) where $\phi_{a,Fe}$ is the anodic potential and ϕ^0 is the equilibrium potential of the redox reaction with a value of -510 mV for Fe→ Fe^{+2} + 2e [20].

Rewriting equation (5), we consider the argument $\beta_{a,Fe} = \frac{RT}{\alpha zF}$ where $\beta_{a,Fe}$ ($Volts^{-1}$) represent the TAFEL anodic constant. The value of $\beta_{a,Fe}$ can be estimated assuming the following values. A symmetry coefficient of polarization α is equivalent to ½, ideal gas constant R = 8.314 $JK^{-1}mol^{-1}$, Faraday´s constant F =96487 C mol^{-1}, the electron exchange number z for iron case Fe→ Fe^{+2} + 2e, z = 2, and T is the interphase temperature assumed Temperature of room. Then, this can be estimated as β^{-1} = 31.97 mV [21], for a cell S-ED/PEC. Therefore, the expression for energy of equation (4) is simplified in equation (6).

$$E_d = \int_0^{ton} V_a * i_{o,Fe} * exp(\eta_{Fe} * \beta^{-1}{}_{a,Fe}) dt \tag{6}$$

Equation (7) is used to calculate the MRR_{hyb} of the SEDCM drilling of low-resistivity in deionized water (LR-DW), where the pulsed duration takes two relevant conditions, namely, i) $\Delta t_{on,ED}$ for the ED condition and ii) $\Delta t_{on,EC}$ for the EC condition. Thus, $t_{on} = \Delta t_{on,ED} + \Delta t_{on,EC}$ is established by the simultaneous condition.

$$MRR_{hyb} t_c = \left(MRR_s^p \, \Delta t_{on,ED} + MRR_d^p \, \Delta t_{on,EC}\right) A_T \tag{7}$$

Substituting equations (1) to (6) for equation (7), the resulting volume of material removed during SEDCM drilling is estimated by equation (8) where MRR_{hyb} is the volume removal rate $[mm^3 \cdot min^{-1}]$ and K_s, K_d are the machinability constants of the subsystems ED and EC, respectively.

$$MRR_{hyb} = \left[\left(\frac{1}{t_c} K_s * E_s(t)\right) + \left(\frac{1}{t_c} K_d * E_d(t)\right)\right] A_T \tag{8}$$

$$A_T = 2\pi * R_m * \delta \tag{9}$$

where A_T (mm^2) is the cutting of the cross-section area, R_m (µm) is the average radius of the tooling and δ (µm) is the tool thickness. The amount of energy for each subsystem, $E_s(t)$ and $E_d(t)$, for a hybrid condition of SEDCM is represented by terms in the equations (3) and (6), which can be solved using an experimental pulsed electrical signal.

2.2 Physical and chemical activation of the surface for simultaneous ED/PEC drilling

The combination of two phenomena, namely, electro-thermal discharge and electro-ionic dissolution, in simultaneous ED/PEC, increases the speed of removal via the physical chemical activation of the metallic surface condition due to an advantage interchange. A conceptual scheme of the removal mechanism for EDM and S-ED/PEC drilling is presented in Figs. 4 and 5. The initial surface condition is $t_{i=0} = 0$, and volume removal is $VR = 0$, as presented in Fig. 4 (a) for ED. After the first discharge condition $t_{i+1} = t_{on,ED}$, the volume $VR_1 = VR_s$ (sparking volume removal), as indicated in Fig. 4 (b). It is known that for each spark produced for EDM, this produces high roughness as reported by Zhao et al. (2013). In Fig. 4 (c) and (d), the second discharge condition is $t_{i+2} =$

$2t_{on,ED}$, and the second volume is defined as: $VR_2 = \varphi VR_s$, where the fraction $\varphi < 1$, $VR_2 < VR_1$ and the volume release is not equal to the first discharge. The simultaneous SEDCM drilling for the ED condition reveals that the initial surface for is $t_{i=0} = 0$ and the $VR = 0$, as in Fig. 5 (a). After the first discharge for the first $\Delta t_{on,ED}$ the volume removal is $VR_{s1} = VR_s$ (Fig. 5 (b)) at $t_{i+2} = \Delta t_{on,EC}$ and there is a change to EC-removal by ion dissolution Fe^{+2}, then the volume $VR_2 = VR_d$ (Fig. 5 (c) and (d)), with a lower roughness surface, as determined by Cheng-Kuang et al. [22]. Then the volume fraction value of $\varphi = 1$, when $VR_{s2} = VR_{s1}$. Following the EC condition, the surface exhibits better behavior due to the amount of material removed by the electro-discharge process. This lower degree of roughness results from the exchange of ions during the electrochemical dissolution of the workpiece.

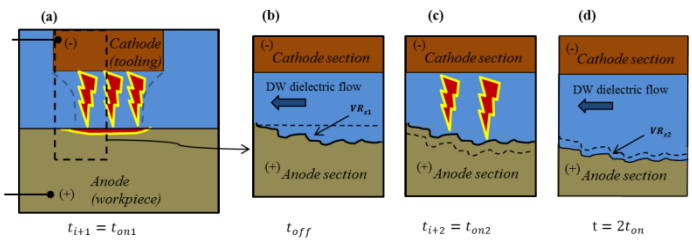

Fig. 4. Scheme of removal mechanism for EDM. (a) Discharge initial, (b) EDM removal of first cycle VR_{s1}, (d) Surface with the relationship of removal volume $VR_{s2} = \varphi VR_{s1}$ for $\varphi < 1$, then $VR_{s2} < VR_{s1}$

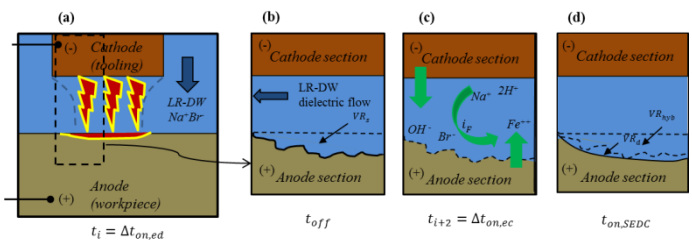

Fig. 5. Removal mechanism for S-ED/PEC (a) Initial discharge ED, (b) ED cycle removal is VR_s, (c) EC cycle removal volume VR_d and (d) S-ED/PEC total cycle of removal volume $VR_{hyb} = VR_s + VR_d$ considered $\varphi = 1$.

2.3 Relationship of material removed volume during EDM and simultaneous ED/PEC drilling

It is possible to determine the fraction contributions of each process for the S-ED/PEC hybrid, where ψ_s (10) is the ED fraction contribution and ψ_d (11) is the EC fraction contribution. The hybrid process can be expressed as $\psi_s + \psi_d = 1$.
Therefore,

$$\psi_s = \frac{VR_s}{VR_s + VR_d} = \frac{K_s E_s}{K_s E_s + K_d E_d} \quad (10)$$

The EC fraction result is

$$\psi_d = \frac{K_d E_d}{K_s E_s + K_d E_d} \quad (11)$$

To determine the machinability constant of simultaneous ED/EC drilling, we use equations (7) and (12) and obtain K_h, which is defined as equation (13):

$$MRR^p * t_c = K_s * E_s + K_d * E_d = K_h * (E_s + E_d) \quad (12)$$

$$K_h = \frac{K_s E_s + K_d E_d}{E_s + E_d} \quad (13)$$

A simplification of equation (8) in terms of machinability constants for the hybrid K_h, the contribution fraction ψ_s of the ED process in equation (10) and the final contribution fraction ψ_d of the EC process in equation (11) results in equation (14). Equation (14) is solved by obtaining the experimental constants for the LR-DW condition of simultaneous ED/EC drilling. Constants in the range of 0.5 to 2.5 MΩ·cm are used to estimate the hybrid machinability constant K_h where the pulsed duration On-time of each constituent ED and EC process are fractions of the On-time condition for S-ED/PEC.

$$MRR_{hyb} = \mathrm{K_h} * A_T \left[\left[\frac{1}{t_c} * \int_0^{ton,ED} (Ie * V)dt \right] + \left[\frac{1}{t_c} \int_0^{ton,EC} [V_a * i_o * \exp(\eta_{Fe} * \beta^{-1}{}_{a,Fe})]dt \right] \right] \quad (14)$$

Using the parametric model correlation proposed that considers the criterion of energy for material removed in a simultaneous ED/EC hybrid as defined by equations 12 to 14, the MRR and the proportion of transferred energy that contributes to each individual process can be determined, as presented in the theoretical scheme of Figs. 4 and 5 for the ED and EC processes, respectively.

3. EXPERIMENTAL

The experiments were performed by adapting the EDM River 300 equipment of Ocean Technologies to obtain a simultaneous ED/EC condition, as presented in Fig. 1. i) The EDM equipment was complemented with two feeder inlets of dielectric and low-resistivity deionized-water (LR-DW). In this configuration, a fluid can be fed in two ways, as displayed in Fig. 2. The EDM feeds the deionized-water as flow F_{in} in the central road through a bronze electrode with an inner diameter of 350 µm, or ii) flow F_{in} with LR-DW NaBr is switched with the second outside flow F_{out} LR-DW NaBr for S-ED/PEC. Sodium bromide salt (1.23 ppm TDS) was used to adjust the

resistivity in 0.5 MΩ · cm to establish a range of 2.1 ± 10 μS·cm^{-1}. The NaBr has the ability to solvate ions and consequently exhibit steady electrical conductivity behavior for high temperatures [23]. The material used for the drilling test was a high strength steel alloy, HSS-550C, which is a cold forming structural material. The chemical composition as specified by the supplier SSAB* is presented in Table 1.

Table 1 Chemical composition of steel HSS-550C wt. % (*)

C	Si	Mn	P	S	Al	Nb	V	Ti	Fe
0.12	0.1	1.8	0.025	0.010	0.015	.09	0.20	0.15	Balance

Samples of 12 x 5 x 16 mm (width x high x large) were cut for milling machining to obtain a homogeneous block. A tubular electrode of 1000 μm outside diameter and 325 μm thickness was used to drill a hole 3 mm in depth. The configuration of the electrode and the workpiece is presented in the diagram of Fig. 2. The experiment was divided in two set conditions. The first experimental condition used only a dielectric medium in DW that measured 2.5 MΩcm at 95°C for EDM, and the other used a low-resistivity dielectric-water measuring 0.5 MΩcm. Both had pressure flows of 600 psi through of tubular electrode. Two regimes of discharge were used during the experiments, namely, 15A and 25A, with duty cycles of 12 to 28 μs, and the amplitude of the pulse was at 30 V and 45 V, respectively, using a square wave pulse train at 25 kHz.

The experimental drilling for SEDCM was performed under a wet regimen with varied conditions for the duty cycle and electrical parameters, as presented in Table 2. The equipment lab was set to ensure that the cycle time of 40 μs was divided proportionally considering an On-time of 28 μm for a 70% duty cycle and an On-time of 12 μs for a 30% duty cycle. This was set for each condition of the current's discharge, low and high, as defined by the measurement of the current using an Oscilloscope Tektronix Mod TDS 2004C 70 MHz,1 GS/s. The processing time begins with the activation of the EDM River 300 equipment and the EDM start-up drilling, and it is recorded at intervals 3 mm depths under conditions of an automatic open circuit. After each test, the samples were cleaned with isopropyl alcohol and with 2% nital at room temperature to reveal the microstructure. The layers were further examined under normal temperatures prior to cutting and after being subjected to heat flow during EDM. Specifically, the white-layer recast and the heat affected layer were measured using a scanning electron microscope, JEOL JSM-6510LV. A Vickers hardness test of the subsurface of the drilling cut drilling was also conducted for each pulsed period under ISO 6507-1:2005 conditions using EMCO-TEST equipment.

Table 2 Experimental DOE test for EDM and simultaneous ED/EC drilling

	On-time (μs)	Ie (A)	Vs (Volts)	Resistivity (MΩ*cm)	Medium
EDM	12,20,28	15	30	2.5	DW
	12,20,28	25	45	2.5	
ED/PEC	12,20,28	15	30	0.5	LR-DW
	12,20,28	25	45	0.5	

4. RESULTS AND DISCUSSION

The performance of the electrical signals for EDM and simultaneous ED/PEC drilling are presented in Fig. 6. A typical electrical signal for the EDM process in the experimental set where the level of DW is 2.5 MΩ·cm is displayed in Fig. 6 (a). This figure displays the results of the transferred energy $E_s(t)$ during the ED cycle. Fig. 6 (b) reveals the results of a signal that was modified for the current in low-resistivity deionized water (LR-DW) and uses a resistivity close to 0.5 MΩ·cm to adjust for the small levels of NaBr. The result is a simultaneous behavior of ED+EC where the current wave was monitored with a decrease in the Faraday current of the EC process using redox electrolysis. This is then divided by the electrical signal in two energy regions where $E_s(t)$ begins the ED process and $E_d(t)$ ends the EC process for each condition duty cycle (DC) of 12 to 28 μs On-time.

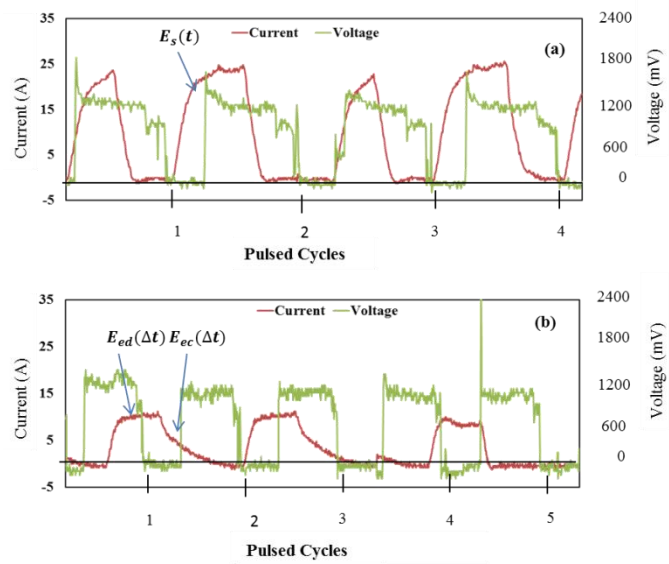

Fig. 6 Performance of electrical signals registered by Oscilloscope (a) EDM signals at 25A with On-time 28 μs and (b) simultaneous ED/PEC at 15A with On-time 20 μs.

The values of transferred energy and machinability shown in Table 3, constants for the MRR_{hyb} theoretical model represented by equation (14) under two power conditions, 25A

and 15A. Equations (1) to (6) yielded the values of transferred energy E_s, E_d and E_{hyb}, whereas machinability constants K_s, K_d, K_h were obtained from equations (8) and (13). Equations (10) and (11) estimate the energy share factor ψ_s for ED and the energy share factor ψ_d for EC, which contribute to S-ED/PEC machining.

Table 3 Transferred energy and machinability constants for the MRR_{hyb} model.

	High Power (25 A/45V)	Low Power (15A/30V)
$\boldsymbol{E_s}$ $[J \cdot cycle^{-1}]$	1125	450
$\boldsymbol{E_d}[J \cdot cycle^{-1}]$	45	27
$\boldsymbol{E_{hyb}}$ $[J \cdot cycle^{-1}]$	1170	477
$\boldsymbol{K_s}$ $[mm^3 \cdot mm^{-2} \cdot J^{-1}]$	4.342x10^{-4}	5.497x10^{-4}
$\boldsymbol{K_d}[mm^3 \cdot mm^{-2} \cdot J^{-1}]$	1.734x10^{-5}	2.180x10^{-5}
$\boldsymbol{K_h}[mm^3 \cdot mm^{-2} \cdot J^{-1}]$	5.070x10^{-4}	6.651x10^{-4}
$\boldsymbol{\psi_s}$	0.924	0.907
$\boldsymbol{\psi_d}$	0.075	0.092

The response of theoretical model is displayed in Fig. 7. A notable difference in the profiles of the MRR for S-ED/PEC and EDM processes was found. Fig. 7 displays an increase in the MRR for EDM when the current and pulse duration increase as reported by Shabgard and Akhbari [24], and Paul and Hiremath [25]. They reported the effect of discharge current and pulse duration for EDM and SEDCM, respectively. In this analysis, it was observed that when the current decays, it is necessary to increase the pulse duration to maintain a constant MRR profile.

The analysis of resistivity for the MRR during S-ED/PEC is show in Fig. 8 with a medium of LR-DW NaBr in the range 0.5 a 2.5 MΩcm at 15A. Fig. 8 (a) is an analysis of the pulsed On-time versus medium resistivity. The MRR exhibits a slight increase under low-resistivity close to the 0.5 MΩcm condition at 12 µs. When resistivity exceeds 1.5 MΩcm as indicated under the EDM condition, a transition point from the EC to the ED condition exists in the simultaneous S-ED/PEC. This is observed in Fig. 8 (b) where, in the region of low voltage, the MRR profile of 8 mm^3/min reveals an inflexion point where the resistivity is above 2.0 MΩcm. This finding is consistent with the results reported by Nguyen et al. [8] expressed that S-ED/PEC has a transition region in the medium of low-resistivity for EC under conditions similar to those of ECM where the system is functioning in low current and low voltage conditions.

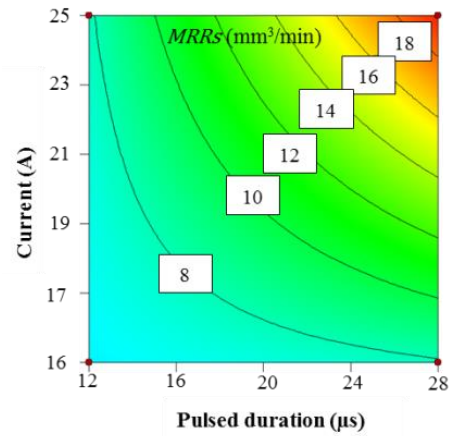

Fig. 7 Analysis material removal rate MRR for EDM at 2.5 MΩcm/45V

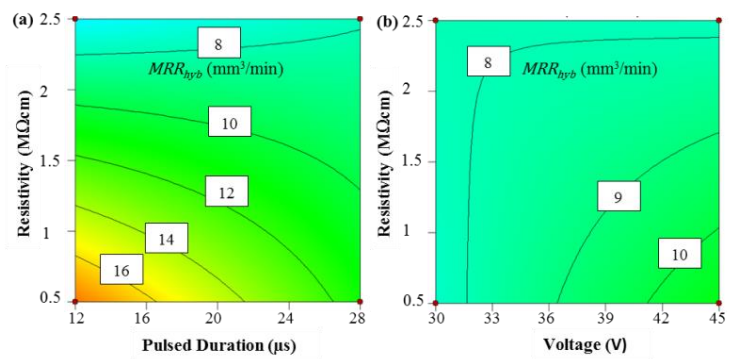

Fig. 8. Analisys of MRR for (a) S-ED/PEC at 15A, 45V and (b) S-ED/PEC at 15A the 12 µs pulsed duration was fixed

Fig. 9 compares the experimental results with the theoretical model of MRR_{hyb} for the MRRs for EDM and simultaneous ED/EC drilling. The MRR_{hyb} is formed by two conditions, ED and EC removal. When the pulsed duration is increased, the effect on both cases is an increase in the material removal rate, as reported Wang et al. [26], who also determined that the effective sparks enable the pulse signal and the subsequent analysis of the mean material removal per discharge. However, the current has the greatest effect on the MRR because the increase in the energy transferred to the workpiece for a long on-time period produces a higher material removal rate. An accelerated MRR behavior of the high current discharge increases by 5 mm^3/min for each 10 µs, whereas the increment for a low current discharge was 2.5 mm^3/min for 10 µs. This is consistent with Klocke et al. [27], who found that the EC has effective material removal rates in the range of 1.51 mm³/(A·min) to 2.13 mm³/(A·min) and that the rate increases as current density increases. The theoretical model presents a good correlation with the experimental data. Even in a low current

condition where the curve exhibits an error higher than the high current, this difference is minimized when the pulse duration increases close to 28 µs. Therefore, in the region of high currents, the effect is due primarily to the ED process because it was conducted in a low-resistivity dielectric medium, and thus, the ED energy share factor ψ_s exhibited a greater influence with a change of 90% at 15A and 92% at 25A. The S-ED/PEC is influenced by the increase in the current associated with the pulse duration and resistivity grade, which results in an increased MRR. The current then affects the value of machinability constants [16].

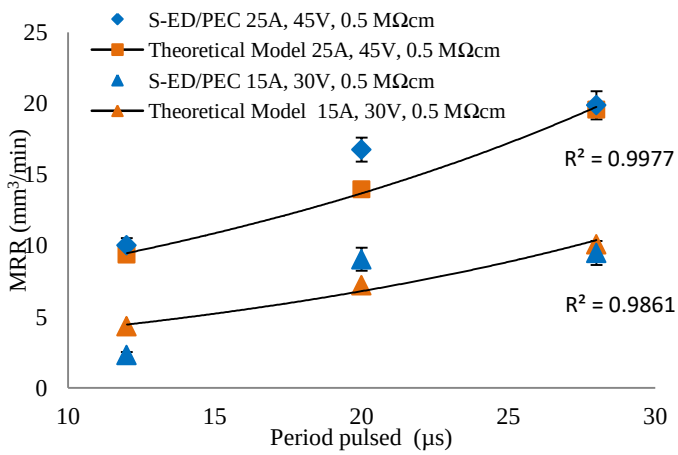

Fig. 9. S-ED/PEC drilling comparison of the MRR experimental versus theoretical model MRR_{hyb}

5. CONCLUSIONS

The analytical correlation of the mathematical model and experimental results of the cutting front for the simultaneous ED/PEC drilling using medium to low-resistivity for drilling in HSS material were established as follows.

- A parametric model proposed for the simultaneous ED/PEC versus the experimental data to determine the MRR was developed with an acceptable correlation close to 0.99 to obtain a machinability constant in the range of 5.07x10^{-4} to 6.65x10^{-4} $[mm^3 \cdot mm^{-2} \cdot J^{-1}]$. The proportion of transferred energy that contributes to individual processes for simultaneous ED/PEC were estimated to be ψ_s = 0.9246 for the ED fraction and ψ_d = 0.0753 for the EC fraction.

- The effect of resistivity on the analysis of response sensibility regarding the material removal rate for simultaneous ED/PEC drilling results in a change of direction of the MRR, specifically, when the resistivity was less than 1.5 MΩ·cm for the PECM contribution at higher voltages with lower current increases slightly the MRR.

The effect of overheating on the EDM process increases the HAZ layer, such that it is six times higher than that of simultaneous ED/PEC drilling of LR-DW. The results indicate that the contribution of PECM allowed the material removal mechanism to reduce the microstructure affectation via assisted dissolution.

Acknowledgments

This work was supported by the CONACYT [Grant numbers 174568 - 2014]

Referencias

[1] K.P. Rajurkar, M.M. Sundaram, A.P. Malshe, Review of Electrochemical and Electrodischarge Machining, ISEM Procedia CIRP 6 (2013) 13 – 26.

[2] P. Pawar, R. Ballav, A. Kumar, Revolutionary Developments in ECDM Process, An Overview 4th International Conference on Materials Processing and Characterization Proceedings 2 (2015) 3188 – 3195.

[3] D. Wang, Z. Zhu, D. Zhu, B. He, H. Ge, Reduction of stray currents in counter-rotating electrochemical machining by using a flexible auxiliary electrode mechanism, Journal of Materials Processing Technology 239 (2017) 66–74.

[4] Q.H. Zhang, J.H. Zhang, S.F. Ren, J.X. Deng, X. Ai, Study on technology of ultrasonic vibration aided electrical discharge machining in gas Journal of Materials Processing Technology, 14th International Symposium on Electromachining ISEM XIV 149 1-3 (2004) 640-644.

[5] H. El-Hofy, Advanced Machining Processes, Non Traditional and Hybrid Machining Processes, Editorial McGraw-Hill, New York, (2005) 220-224.

[6] T. Singh and A. Dvivedi, Developments in electrochemical discharge machining: A review on electrochemical discharge machining, process variants and their hybrid methods, International Journal of Machine Tools and Manufacture 105 (2016) 1–13.

[7] M.D. Nguyen, M. Rahman, Y.S. Wong, Simultaneous micro-EDM and micro-ECM in low-resistivity deionized water. International Journal of Machine Tools and Manufacture 54 (2012) 55–65.

[8] M.D. Nguyen, M. Rahman, Y.S. Wong, Transitions of micro-EDM/SEDCM/ micro-ECM milling in low-resistivity deionized water, International Journal of Machine Tools and Manufacture 69 (2013) 48–56.

[9] G.N. Levy and F. Maggi, WED Machinability Comparison of Different Steel Grades, Annals of CIRP 39 1 (1990) 183-186.

[10] X. Xiao-lei, Y. Zhi-wei, G. Yu-zhou, Micro-cracks on electro-discharge machined surface and the fatigue failure of a diesel engine injector, Engineering Failure Analysis 32 (2013) 124–133.

[11] W. Zhao, L. Gu, H. Xu, L. Li, X. Xiang, A novel high efficiency electrical erosion process - Blasting erosion arc machining. Seventeenth International Symposium on Electro-machining, Procedia CIRP 6 (2013) 621 – 625.

[12] T.R. Newton, S.N. Melkote, T.R. Watkins, R.M. Trejo, L. Reister, Investigation of the effect of process parameters on the formation and characteristics of recast layer in wire-EDM of Inconel 718, Material Science Engineering A 513–514 (2009) 208–215.

[13] Y. Zhang, Z. Xu, J. Xing, D. Zhu, Effect of tube-electrode inner diameter on electrochemical discharge machining of nickel-based superalloy C, Journal of Aeronautics, 29 4 (2016) 1103–1110.

[14] Y. Cheng-Kuang, W. Kun-Ling, H. Jung-Chou, L. Shin-Min, L. Jui-Che, Y. Biing-Hwa,. Enhanement of ECDM efficiency and accuracy by spherical tool electrode, International Journal of Machine Tools and Manufacture 51 (2011) 528–535.

[15] J. Kozak, K.P. Rajurkar, Y. Makkar, Selected problems of micro-electrochemical machining, Journal of Materials Processing Technology 149 (2004) 426–431.

[16] J. Kozak, D. Gulbinowicz, Z. Gulbinowicz , The mathematical modeling and computer simulation of pulse electrochemical micromachining, AIP Conference Proceedings 1127 (2009) 174.

[17] F. Vasca, Dynamic and control of switched electronic systems, Advanced perspectives for modeling, simulation and control of power converters, Editorial Lanelli (2012) 494-496.

[18] J. Tao, J. Ni, A.J. Shih, Modeling of the anode crater formation in electrical discharge machining, Journal Manufacture Science Engineering 134 011002 (2012)1-9.

[19] R. Graver, P.J. Moreland, A literature review of polarization resistance constant (B) values for the measurement of corrosion rate, NACE, Houston (1985).

[20] L.L. Shreir, Electrochemical Principles of Corrosion, A Guide for Engineers, Department of Industry Ed London, Department of Industry (1982) 201-226.

[21] R.R. Winston, Uhlig's Corrosion Handbook, 2nd Ed, Electrochemical Society Series, New York (2000).

[22] Y. Cheng-Kuang, C. Chih-Ping, M. Chao-Chuang, W.A. Cheng , H. Jung-Chou, Y. Biing-Hwa, Effect of surface roughness of tool electrode materials in ECDM performance, International Journal of Machine Tools and Manufacture 50 (2010) 1088–1096.

[23] P.B Bhargav, V.M. Mohan, A.K. Sharma, V.V.R.N. Rao, Structural and electrical properties of pure and NaBr doped poly (vinyl alcohol) (PVA) polymer electrolyte films for solid state battery applications, Journal Ionics 13 (2007) 441–446.

[24] M. Shabgard and S. Akhbari, An inverse heat conduction method to determinate the energy transferred to the work piece in EDM process, International Journal Advanced Manufacture Technology 83 (2016) 1037–1045.

[25] L. Paul and S.S. Hiremath, Response Surface Modelling of Micro Holes in Electrochemical Discharge Machining Process Icon DM, Procedia Engineering 64 (2013) 1395 – 1404.

[26] J. Wang, F. Yang, J. Qian, D. Reynaerts, Study of alternating current flow in micro-EDM through real-time pulse counting, Journal of Materials Processing Technology 231(2016) 179–188.

[27] F. Klocke, M. Zeis, A. Klink, D. Veselovac, Experimental research on the electrochemical machining of modern titanium- and nickel-based alloys for aero engine components, The Seventeenth CIRP Conference on Electro Physical and Chemical Machining (ISEM) (2013) 368 – 372.